Predicted Rupture Force of a Single Molecular Bond Becomes Rate Independent at Ultralow Loading Rates

Dechang Li and Baohua Ji[*]

Biomechanics and Biomaterials Laboratory, Department of Applied Mechanics, Beijing Institute of Technology, Beijing 100081, China

We present for the first time a theoretical model of studying the saturation of the rupture force of a single molecular bond that causes the rupture force to be rate independent under an ultralow loading rate. This saturation will obviously bring challenges to understanding the rupture behavior of the molecular bond using conventional methods. This intriguing feature implies that the molecular bond has a nonzero strength at a vanishing loading rate. We find that the saturation behavior is caused by bond rebinding when the loading rate is lower than a limiting value depending on the loading stiffness.

PACS numbers: 82.37.Np, 87.15.A-

Single-molecule dynamic force spectroscopy (DFS) has been proved a powerful tool in obtaining information on the intrinsic properties of molecular systems [1–3]. For instance, it allows us to extract the properties of the energy landscape of molecular interaction (e.g., energy barrier ΔG_{off}, width of the energy well x_β and dissociation rate constant k_{off}) through the relationship between the rupture force and loading rate by Bell- or Kramer-like relations [4]. But there have been considerable arguments about the applicability of these classical relations regarding the range of pulling rates and device stiffness. These relations may not be valid at relatively low loading rate; e.g., they might not be applicable when the loading rate Kv (K the device stiffness, v the pull velocity) is lower than ~ 10 pN/s for a typical energy landscape with $k_{off} \sim 1$ s^{-1} and $x_\beta \sim 0.5$ nm [5]. However, the loading devices in many DFS experiments, e.g., laser optical tweezers and magnetic tweezers, often have a much lower loading rate, as low as $10^{-3} - 10^1$ pN/s [6–8]. Similarly, under physiological conditions, the loading rate of a receptor-ligand separation was also as low as $0.5 - 5$ pN/s for a typical molecule pair (e.g., the avidin–biotin pair [5]) with a classical molecular stiffness of $1 - 10$ pN/nm [9]. These facts challenge the applicability of conventional methods in studying the single molecular interaction at physiological conditions, such as those in biomedical engineering.

The rupture behaviors of molecular bonds at the ultralow loading rates have recently received intensive attention [7,8,10–13] because of its scientific importance as well as its distinct features compared with those at the faster loading rates. It was observed that many so-called "mechanical" proteins (e.g., fibronectin and titin) exhibited a nonzero asymptotic strength limit of unfolding at a vanishing loading rate [11,14,15]. Recent experiments showed that at the ultralow loading rates, the mean rupture force of single receptor-ligand bond exhibits a similar asymptotic manner

[7,16,17]. These asymptotic behaviors immediately challenge the conventional understanding of the strength of a molecular bond that is believed to be rate dependent and to diminish to zero at a vanishing loading rate. Those observations thus raise the question of how to understand the rupture behaviors of a molecular bond at an ultralow loading rate. Recent modeling activities [18–22], however, mainly focus on the effect of the loading stiffness. There is no theoretical model on the bond strength at the ultralow loading rate. Currently, several fundamental questions remain to be understood, e.g., what are the differences of the rupture behaviors of the molecular bond under an ultralow loading rate in comparison with those under a high loading rate, how to estimate the critical loading rate below which the conventional methods may fail, and how to improve the DFS analysis dominated by the conventional methods. This work is to pursue these questions by using both theoretical analyses and Brownian dynamic (BD) simulations. Our results show that it is the bond rebinding that causes the saturation of bond strength at ultralow loading rates, which immediately suggests a nonzero strength of a molecular bond even at the vanishing loading rate. A new theory is developed for designing and analyzing the DFS experiments and simulations at ultralow loading rates.

Here, we treat the force-induced bond rupture as a thermally activated escape of a particle (A) over a single energy barrier that is perturbed by an external force (see Fig. 1). The energy landscape of the single-molecule system is illustrated in Fig. 1(a), where ΔG_{on} and ΔG_{off} are the energy barriers for association and dissociation, respectively, and x_β is the width of energy well. Because ΔG_{on} is normally very small (e.g., ~ 5 $k_B T$) in comparison with ΔG_{off}, for the convenience of the analysis, we neglect the effect of ΔG_{on} so that the energy landscape can be modeled by a harmoniclike potential that is harmonic for $x < x_\beta$, but becomes flat when $x > x_\beta$ (dashed line
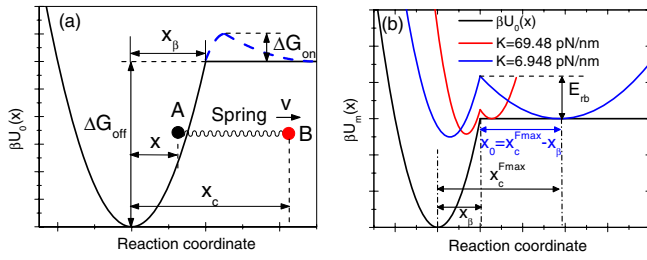
FIG. 1 (color online). Illustration of the energy landscape of the single molecule bond. (a) A single well energy landscape, where x_β is the width of energy well, x is the position of particle A, and x_c is the position of dummy particle B. The part of the energy landscape in the blue dashed line is simplified to a plateau of the landscape at $x > x_\beta$, neglecting the effect of ΔG_{on} for the convenience of analytical analysis. (b) Illustration of the intrinsic energy landscape (in black) as well as the combined energy landscape tilted by the loading device at two different loading stiffness (in blue and red). $x_c^{F\,max}$ is the critical position of the dummy particle B for bond rupture. E_{rb} is the energy barrier of the combined system for bond rebinding.

becomes solid line). An external force is applied on a dummy particle (B) via a harmonic spring of stiffness K which mimics the pulling device. The free energy of the combined system consisting of the particle and the pulling spring can be expressed by

$$\beta U_m(x,t) = \beta U_0(x,t) + \frac{1}{2}K[x - x_c(t)]^2, \quad (1a)$$

and

$$\beta U_0(x,t) = \begin{cases} \Delta G_{off}\left(\dfrac{x}{x_\beta}\right)^2 & -\infty < x \le x_\beta, \\ \Delta G_{off} & x_\beta < x < \infty \end{cases} \quad (1b)$$

where $\beta = (k_B T)^{-1}$, k_B is Boltzmann constant and T is absolute temperature. The term $(1/2)K(x - x_c)^2$ is the elastic energy stored in the pulling spring, while $x_c(t) = vt$ is the displacement of dummy particle at time t, and v is the pulling speed. The energy landscape of the combined system is illustrated in Fig. 1(b). Note that the effective stiffness of the combined system is $K_{eff} = K_0 K/(K_0 + K)$ [19], where $K_0 = 2\Delta G_{off}/x_\beta^2$ is the intrinsic stiffness of the molecular interaction. In this Letter, for the convenience of a comparison with DFS experiments, we use Kv as the apparent loading rate in the plot of results.

Different from previous works [18–21], here, we study the bond rupture at an ultralow loading rate by considering the bond rebinding. The ultralow loading rate denotes the pulling rate at which the bond rebinding dominates the rupture behaviors. Previous models based on Kramers' description of irreversible rupture did not take into account the rebinding effect [18–21]. Therefore, the rupture force calculated by those models is different—the rupture of a molecular bond happens once the position of particle A
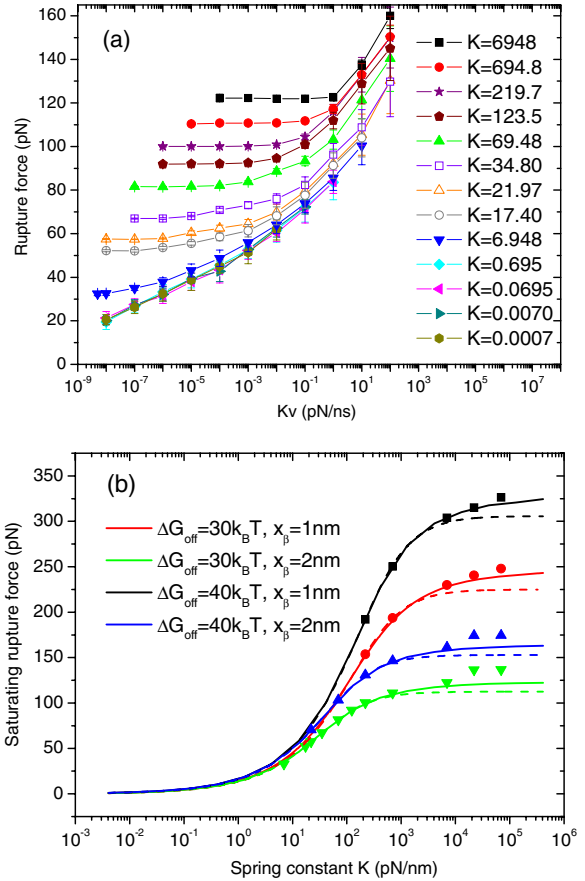

FIG. 2 (color online). (a) The mean rupture force obtained from the BD simulations for a different spring constant K, with $\Delta G_{off} = 30 \ k_B T$, $x_\beta = 2$ nm. The unit of the spring constant K is pN/nm. (b) The relationship between the saturating rupture force and the stiffness of the loading device K. The solid and dashed lines are for the numerical and analytical solutions of Eq. (5), respectively, and the symbols are for the results of the BD simulations.

satisfies $x = x_\beta$, and the bond rebinding is not considered. In contrast, in this study, the rupture can happen at a position $x > x_\beta$ with multiple times of bond rebinding, which enhances the rupture strength of a molecular bond.

The rupture process of the particle A being pulled out of the energy well is firstly simulated using the BD simulations (more simulation details are given in the text S1 and Fig. S1 in the Supplemental Material [23]). The results show that the rupture force decreases with reducing the loading rate. In addition, the slope of the $\langle F \rangle_{max} \sim \ln(Kv)$ plot also decreases with the loading rate. When the loading rate is reduced to below a critical value, the rupture force becomes rate independent, see Fig. 2(a). This result is consistent with recent experiments [7,11,14–17] showing that there are asymptotic strength limits for the rupture of a single receptor-ligand bond as well as the unfolding of β-sheet-rich proteins at the ultralow loading rates. It thus suggests a nonzero strength of a molecular bond even at a vanishing loading rate, which is different from previous studies [18–21]. In this Letter, we call the asymptotic strength limit value as the saturating rupture force. Note that the saturating

rupture force increases with the loading stiffness and can be significant at a high stiffness. We also found that the slower the loading rate, the more significant the rebinding effect on the rupture process. Figure S2 depicts typical force traces obtained from three different loading rates [23]. These results suggest that the rebinding takes a more dominant role in the bond rupture behavior at the ultralow loading rate.

To study the effect of rebinding on the rupture force, we will first derive the mean position of a particle A for calculating the pulling force. Based on the BD simulation results, we assume that the rate of relaxation of the particle A is much faster than the velocity of the dummy particle B as long as the pulling rate is sufficiently slow. As a result, particle A can have enough time to travel to all of the possible positions in the energy landscape driven by thermal fluctuation. Thus, the partition function Z of the system at time t is given by $Z = \int_{-\infty}^{\infty} \exp[-\beta U_m(x, t)]dx$, and the probability of particle A appearing at position x is $p(x) = (1/Z) \exp[-\beta U_m(x, t)]$. Our BD simulation results fully support this assumption that when the pulling velocity is sufficiently slow, particle A has the possibility to travel back to the energy well after its escape, which then induces the rebinding of the molecular bond (Fig. S2) [23]. Thus, the average position of particle A is obtained as $\langle x \rangle = \int_{-\infty}^{\infty} xp(x)dx$. By plugging the expression of $p(x)$ into $\langle x \rangle$, we have

$$\langle x \rangle = x_c \frac{\frac{1}{\xi^2} + \xi \exp\left[\left(\frac{x_c^2}{x_\beta^2 \xi^2} - 1\right)\Delta G_{\text{off}}\right]}{1 + \xi \exp\left[\left(\frac{x_c^2}{x_\beta^2 \xi^2} - 1\right)\Delta G_{\text{off}}\right]}, \quad (2)$$

where $\xi = \sqrt{\frac{2\Delta G_{\text{off}} + Kx_\beta^2}{Kx_\beta^2}}$. According to Eq. (2), we can obtain the mean force determined by the extension of the spring at the ultralow loading rate as

$$\langle F \rangle = K(x_c - \langle x \rangle). \quad (3)$$

By applying $(d\langle F \rangle/dx_c) = 0$, we obtain the critical position of the dummy particle B for the maximum value of the mean force (i.e., the rupture force) as

$$x_c^{F\,\text{max}} = x_\beta \sqrt{\frac{\xi^2}{\Delta G_{\text{off}}} \left\{ \text{Lambert}\,W\left[\frac{\exp(\Delta G_{\text{off}} - \frac{1}{2})}{2\xi}\right] + \frac{1}{2}\right\}}. \quad (4)$$

where Lambert $W(x)$ is the Lambert W function that satisfies the condition Lambert $W(x) \times \exp[\text{Lambert}\,W(x)] = x$. Thus, the rupture force at ultralow loading rate is obtained as

$$\langle F \rangle_{\text{max}} = K(x_c^{F\,\text{max}} - \langle x \rangle^{F\,\text{max}})$$

$$= \frac{K\left(1 - \frac{1}{\xi^2}\right)}{1 + \xi \exp\left\{\left[\left(\frac{x_c^{F\,\text{max}}}{x_\beta \xi}\right)^2 - 1\right]\Delta G_{\text{off}}\right\}} x_c^{F\,\text{max}}. \quad (5)$$

where $\langle x \rangle^{F\,\text{max}}$ is calculated by substituting Eq. (4) into Eq. (2).

Figure 2(b) shows the comparison between the BD simulations and the theoretical predictions of saturating rupture forces in terms of spring constants of pulling device. The theoretical predictions agree well with those of the BD simulations. Note that the saturating rupture force increases with the probe stiffness in a nonlinear fashion. This is a new finding of the effect of the loading stiffness on the rupture force which is different from the one found in previous studies at a high loading rate [18–21]. They showed that the increase of loading stiffness reduces the bond dissociation rate, which results in the increase of the rupture force. Here, we show below that besides that mechanism, the increase of the loading stiffness will further increase the rupture force at the ultralow loading rate because of its effect on bond rebinding. Tshiprut et al. [18] had shown in their simulations that the stiffness of the loading device can influence the bond rebinding dynamics. In particular, we show that the saturating rupture force is also a function of ΔG_{off} and x_β [see Fig. 2(b)]. This result suggests a new method of extracting the properties of the energy landscape by measuring the saturating rupture force at a different loading stiffness and then calculating ΔG_{off} and x_β using Eq. (5) (Table S1 in the Supplemental Material [23]).

We also find that the higher the pulling stiffness, the higher the critical loading rate at which the saturation appears, according to Fig. 2(a). This phenomenon can be understood by studying the effect of the pulling stiffness on the energy barrier for rebinding as follows. The energy barrier for the rebinding is given by [see illustration in Fig. 1(b)]

$$E_{rb}$$

$$= \frac{1}{2}K(x_c^{F\,\text{max}} - x_\beta)^2$$

$$= \frac{1}{2}Kx_\beta^2 \left(\sqrt{\frac{\xi^2}{\Delta G_{\text{off}}}\left\{\text{Lambert}\,W\left[\frac{\exp(\Delta G_{\text{off}} - \frac{1}{2})}{2\xi}\right] + \frac{1}{2}\right\}} - 1\right)^2. \quad (6)$$

Figure 3 depicts the energy barrier E_{rb} as a function of the spring constant, in which the relationship between $x_c^{F\,\text{max}}$ and the spring constant is also illustrated. Note that the lower the spring stiffness K, the higher the energy barrier that the particle A needs to overcome for the rebinding. This result seems to be counterintuitive because when the spring stiffness is lower, it should be easier for particle A to rebind as there is less restriction from the softer spring. How to understand this behavior? According to Eq. (4), $x_c^{F\,\text{max}}$ is
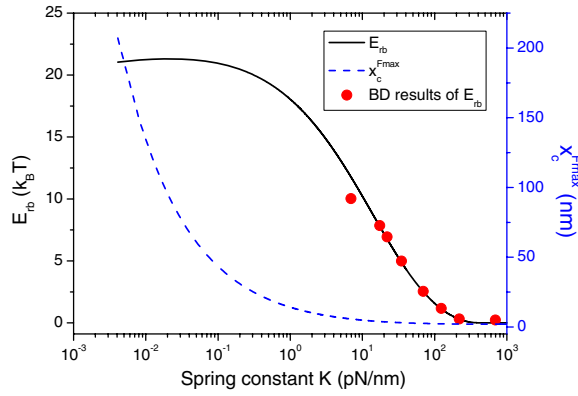
FIG. 3 (color online). Predictions of the energy barriers E_{rb} for the bond rebinding and the critical position of dummy particle B $x_c^{F\,\max}$ for the bond rupture at different spring constants. The red circular symbols are for the results of BD simulations. $\Delta G_{\text{off}} = 30\,k_B T$ and $x_\beta = 2$ nm.

FIG. 4 (color online). Predictions of the limiting loading rate Kv_{rb} and the first passage time t_K for bond rebinding at different spring constants K. The red circular symbols are for the results of the BD simulations. $\Delta G_{\text{off}} = 30\,k_B T$ and $x_\beta = 2$ nm.

approximately proportional to $\sqrt{1/K}$ (see text S2 in the Supplemental Material [23]). Substituting this relationship into Eq. (6) and considering $x_c^{F\,\max} - x_\beta > 0$, we can immediately prove that the energy barrier increases with the decease of spring stiffness. The mechanism is that when the spring stiffness is decreased, the particle A needs to travel a longer distance (i.e., $x_c^{F\,\max} - x_\beta$) for rebinding and therefore, has less possibility to rebind. In order to make it possible, it requires a slower loading so that the particle A has enough time for the rebinding. Therefore, the smaller the K value, the lower the loading rates for the saturation of the rupture force [see also Fig. 2(a)].

The stiffness dependent rupture force of a receptor-ligand bond may be related to the mechanosensitivity of the cell adhesion to the stiffness of extracellular matrix (ECM); e.g., cells prefer to spread and form stable adhesion at a stiff substrate [24–27]. Because the stiffness of substrate is one of the main contributors to the loading stiffness of receptor-ligand bonds in cell adhesion, the stiff substrate will facilitate the receptor-ligand rebinding, while the soft one will suppress it [24,25]. As a result, the receptors and ligands would form stronger bonds at the stiffer substrate for a more stable cell adhesion compared with the softer one. This Letter provides further evidence for the mechanosensitivity of cell adhesion from the molecular level.

On the other hand, the saturation of rupture force will, however, bring challenges to DSF analysis using prior theories. For example, we find that they will not be valid when $Kv < (k_{\text{off}}/x_\beta)\exp(\gamma)$, where $\gamma \approx 0.577$ is the Euler constant [4]. Therefore, it is crucial to identify the critical loading rate at which the saturation will occur before we decide whether prior theories could be applied. In order to estimate the threshold value of the loading rate, we need first to estimate the first passage time of particle A for rebinding, i.e., the time for its moving back to the energy well once it is pulled out. The first passage time t_K is defined as the mean time for a particle to diffuse toward a distance
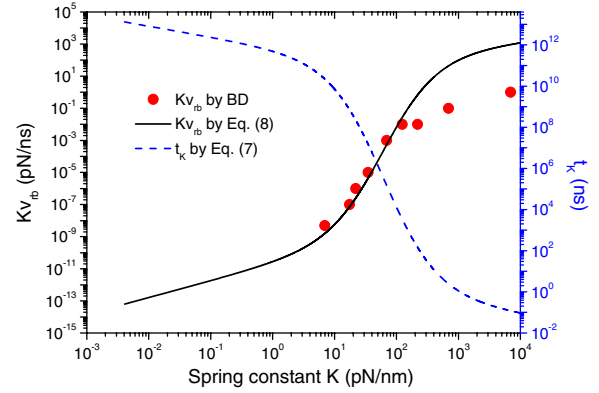
$x_0 = x_c^{F\,\max} - x_\beta$ in the energy well, which defines the time scale for the rebinding of particle A. For a harmonic potential which satisfies $\frac{1}{2}Kx_0^2 \gg 1$, the first passage time can be estimated as (see text S3 in the Supplemental Material [23])

$$t_K = \frac{1}{D}\sqrt{\frac{2\pi}{K}}\left(\frac{1}{K(x_c^{F\,\max} - x_\beta)}\right)\exp\left(\frac{K(x_c^{F\,\max} - x_\beta)^2}{2}\right).$$

(7)

Thus, we can estimate the critical loading rate for rebinding as,

$$Kv_{rb} = K\frac{x_c^{F\,\max} - x_\beta}{t_K}.$$

(8)

When the loading rate satisfies $Kv \leq Kv_{rb}$, i.e., being the ultralow loading rate, the rebinding may cause saturation of the rupture force. Figure 4 depicts the changing of the first passage time t_K and the critical loading rate Kv_{rb} as functions of a spring constant K, showing a good agreement between the theoretical predictions and BD simulations. The smaller the spring constant K, the more time the particle A needs for the rebinding, and thus, the lower the critical loading rate [see also Fig. 2(a)]. For example, Chen et al. [28] measured the unfolding force of Filamin A rod segments using magnetic tweezers which has a stiffness around 10^{-6} pN/nm [29]. In this case, the critical loading rate for the saturation of the unfolding forces should be as low as 10^{-8} pN/s. This is the reason that the unfolding force always depends on the loading rates in the range from 0.2 pN/s to 20 pN/s in Chen et al. experiment [28]. It is expected that when the stiffness of the pulling device approaches zero, rebinding should be prohibited. This behavior is opposite to the case where the pulling device has a high stiffness, which confines the locations of the particle A and therefore, allows rebinding to happen. This also implies that the traditional Bell- or Kramer-like relations should be still applicable to the experiments using magnetic tweezers.

Knowledge of the critical loading rate Kv_{rb} is crucial to the DFS analysis. On one side, it can help improve the predictions of DFS analysis. For example, because the rebinding effect can significantly influence the slope of $\langle F \rangle_{max} \sim \ln(Kv)$ plot, previous theories [4] may not correctly predict the properties of the energy landscape by simply fitting the plot when the loading rate is smaller than Kv_{rb} [see Eq. (8)]. Therefore, a data filtration (to filter out the data with bond rebinding) is needed to improve the accuracy of predictions (see Table S1 in the Supplemental Material [23]). Table S1 shows that for a higher loading stiffness, when there are more data obtained at the ultralow loading rate, there are big errors in the predictions by direct fitting, and the filtration significantly improves the predictions. On the other side, the knowledge of Kv_{rb} will also provide guidelines for choosing the spring constant of a loading device and a loading rate in DFS experiments to reduce the rebinding effect. For a stiff loading device, one should choose a fast loading. However, for a soft device, one can choose a slow one.

In conclusion, we have studied the saturation of the rupture force which is a new feature of the single receptor-ligand bond that was not found before. We showed that when the loading rate was smaller than a critical value, the rupture force became no longer dependent on the loading rate, which implies a nonzero strength of a molecular bond at a quasistatic loading. We found that this saturation behavior was caused by a bond rebinding at the ultralow loading rate. We further derived an analytical solution of the limiting loading rate below which the bond rebinding dominates the rupture process, which is found to increase with the stiffness of loading device. This solution will assist us to determine which DFS data are valid for calculating the properties of an energy landscape by fitting the $\langle F \rangle_{max} \sim \ln(Kv)$ plot using conventional methods, and thus, to highly improve the predictions. It would also provide guidelines for preparing DFS experiments and simulations on how to choose the loading rates according to the stiffness of loading devices. More importantly, we also suggested a new way to design DFS experiments by measuring the saturating rupture force at different loading stiffness, by which one can accurately calculate the parameters of energy landscapes of a molecular bond.

*Corresponding author.
bhji@bit.edu.cn

[1] S. Kumar and M. S. Li, Phys. Rep. **486**, 1 (2010).
[2] E. Evans, Annu. Rev. Biophys. Biomol. Struct. **30**, 105 (2001).
[3] T. Hugel and M. Seitz, Macromol. Rapid Commun. **22**, 989 (2001).
[4] O. K. Dudko, G. Hummer, and A. Szabo, Phys. Rev. Lett. **96**, 108101 (2006).
[5] J.-M. Teulon, Y. Delcuze, M. Odorico, S.-W. Chen, P. Parot, and J.-L. Pellequer, J. Mol. Recognit. **24**, 490 (2011).
[6] R. Merkel, P. Nassoy, A. Leung, K. Ritchie, and E. Evans, Nature (London) **397**, 50 (1999).
[7] Y. Zhang, G. Sun, S. Lü, N. Li, and M. Long, Biophys. J. **95**, 5439 (2008).
[8] M. Panhorst, P.-B. Kamp, G. Reiss, and H. Brückl, Biosens. Bioelectron. **20**, 1685 (2005).
[9] B. T. Marshall, K. K. Sarangapani, J. Wu, M. B. Lawrence, R. P. McEver, and C. Zhu, Biophys. J. **90**, 681 (2006).
[10] S. Breisch, J. Gonska, H. Deissler, and M. Stelzle, Biophys. J. **89**, L19 (2005).
[11] S. Keten and M. J. Buehler, Phys. Rev. Lett. **100**, 198301 (2008).
[12] D. Li, B. Ji, K.-C. Hwang, and Y. Huang, PLoS One **6**, e19268 (2011).
[13] D. Li and B. Ji, Acta Mechanica Sinica **28**, 891 (2012).
[14] J. I. Sulkowska and M. Cieplak, J. Phys. Condens. Matter **19**, 283201 (2007).
[15] M. Sotomayor and K. Schulten, Science **316**, 1144 (2007).
[16] F. R. Kersey, D. M. Loveless, and S. L. Craig, J. R. Soc. Interface **4**, 373 (2007).
[17] A. Ptak, M. Kappl, S. Moreno-Flores, H. Gojzewski, and H.-J. Butt, Langmuir **25**, 256 (2009).
[18] Z. Tshiprut, J. Klafter, and M. Urbakh, Biophys. J. **95**, L42 (2008).
[19] A. Maitra and G. Arya, Phys. Rev. Lett. **104** (2010).
[20] E. B. Walton, S. Lee, and K. J. V. Vliet, Biophys. J. **94**, 2621 (2008).
[21] G. Yoon, S. Na, and K. Eom, J. Chem. Phys. **137**, 025102 (2012).
[22] Z. Tshiprut and M. Urbakh, J. Chem. Phys. **130**, 084703 (2009).
[23] See Supplemental Material at http://link.aps.org/supplemental/10.1103/PhysRevLett.112.078302 for simulation methods, theoretical derivations and supporting figures and tables.
[24] J. Qian, J. Wang, Y. Lin, and H. Gao, Biophys. J. **97**, 2438 (2009).
[25] J. Qian and H. J. Gao, PLoS One **5**, e12342 (2010).
[26] D. Kong, B. Ji, and L. Dai, Biophys. J. **95**, 4034 (2008).
[27] D. Kong, B. Ji, and L. Dai, J. Biomech. **43**, 2524 (2010).
[28] H. Chen, X. Zhu, P. Cong, M. P. Sheetz, F. Nakamura, and J. Yan, Biophys. J. **101**, 1231 (2011).
[29] K. C. Neuman and A. Nagy, Nat. Methods **5**, 491 (2008).